Flood mapping using VHR satellite imagery: a comparison between different classification approaches

Flood mapping using VHR satellite imagery: a comparison between different classification approaches

Francesca Franci*[a], Piero Boccardo[b], Emanuele Mandanici[a], Elena Roveri[a], Gabriele Bitelli[a]
[a]DICAM, University of Bologna. Viale Risorgimento 2, Bologna, Italy;
[b] DIST, Politecnico di Torino, Viale Matteoli 39, Torino, Italy.

ABSTRACT

Various regions in Europe have suffered from severe flooding over the last decades. Flood disasters often have a broad extent and a high frequency. They are considered the most devastating natural hazards because of the tremendous fatalities, injuries, property damages, economic and social disruption that they cause.

In this context, Earth Observation techniques have become a key tool for flood risk and damage assessment. In particular, remote sensing facilitates flood surveying, providing valuable information, e.g. flood occurrence, intensity and progress of flood inundation, spurs and embankments affected/threatened.

The present work aims to investigate the use of Very High Resolution satellite imagery for mapping flood-affected areas. The case study is the November 2013 flood event which occurred in Sardinia region (Italy), affecting a total of 2,700 people and killing 18 persons. The investigated zone extends for 28 km^2 along the Posada river, from the Maccheronis dam to the mouth in the Tyrrhenian sea.

A post-event SPOT6 image was processed by means of different classification methods, in order to produce the flood map of the analysed area. The unsupervised classification algorithm ISODATA was tested. A pixel-based supervised technique was applied using the Maximum Likelihood algorithm; moreover, the SPOT 6 image was processed by means of object-oriented approaches.

The produced flood maps were compared among each other and with an independent data source, in order to evaluate the performance of each method, also in terms of time demand.

Keywords: Flood mapping, Sardinia, object-based classification, pixel-based classification, disaster management, SPOT 6, 2013 flood event.

1. INTRODUCTION

In many EU countries, consequences of flooding events have been getting heavier and heavier over time, in terms of the damages and losses of lives being caused[1]. They are considered the most devastating natural hazard because of the tremendous fatalities, injuries, property damages, economic and social disruption that they cause[2]. Therefore, extracting and evaluating flooded areas timely and rapidly is essential for decreasing the losses[3].

Several studies have been elaborated on the importance and applications of remote sensing data, with particular reference to satellite images, in the field of disaster risk management[4,5,6]. Remote sensing based analyses are nowadays frequently adopted to support both decision makers and first responders during disaster management activities[7]. A major reason for using remote sensing consists in the fact that it is the fastest means of data collection for pre- and post-event disaster studies[8]. In fact, rapid mapping activities for supporting the first stage of disaster management are frequently based on satellite remote sensing data.

This is true also for flood risk management, where Earth Observation techniques have become a key tool for both prevention and damage assessment, supporting flood surveying and providing valuable information, e.g. flood occurrence, intensity and progress of flood inundation, spurs and embankments affected/threatened[9,10,11]. Very high spatial resolution visible and near-infrared satellite data can be used for a wide range of applications and operations during and after natural disasters[12]; they can be coupled or integrated by SAR imagery analysis.

*francesca.franci2@unibo.it; phone +39 051 2093109; fax +39 051 2093114

Earth Resources and Environmental Remote Sensing/GIS Applications VII, edited by Ulrich Michel, Karsten Schulz, Manfred Ehlers, Konstantinos G. Nikolakopoulos, Daniel Civco, Proc. of SPIE Vol. 10005, 1000509
© 2016 SPIE · CCC code: 0277-786X/16/$18 · doi: 10.1117/12.2241390

The present work aims to investigate the use of Very High Resolution (VHR) optical satellite imagery for mapping flood-affected areas. The case study is the November 2013 flood event which occurred in Sardinia region (Italy), affecting a total of 2,700 people and killing 18 persons. The adopted imagery is from SPOT 6 platform.

Different classification methods were evaluated in order to produce the flood map of the analysed area. In the perspective of emergency management, the rapid identification of flood boundaries is crucial to effectively conduct the response activities, e.g. evacuation, rescue and needs assessment. Therefore, the unsupervised classification algorithm ISODATA was tested. A pixel-based supervised technique was then applied using the Maximum Likelihood (ML) algorithm; moreover, the VHR image was processed by means of an object-oriented approach.

All the flood maps, produced using supervised and unsupervised classification procedures, were compared among each other and with an independent dataset in terms of detected flooded areas and processing time.

2. CASE STUDY

2.1 2013 Sardinia flood event

Cyclone Cleopatra (also called Ruven) passed through Sardinia region (Italy) during the night of November 18, 2013, causing severe flooding, substantial damage to infrastructures and several casualties across the island. About 2,700 people were evacuated, 18 casualties were reported and one person is still missing. The city and province of Olbia in Sardinia's northeast were among the most severely affected areas.

The study area is located along the Posada river, between Maccheronis dam and the river mouth in the Tyrrhenian sea. It covers about 28 km^2. River meanders are characterized by intensive farming (greenhouses and vegetable gardens). Tourist facilities and seaside resorts rise in the coastal areas. The main villages are located on the right bank of river: Torpé and Posada (Figure 1).

This zone is subject to flooding; therefore, almost half of the river length is controlled by 4 m height embankments. During the cyclone overpass, intense rains and heavy flows caused the dam overtopping (enlarging works for increasing the reservoir volume had been suspended); downstream, the river flood wave caused severe damages to the embankments resulting in widespread flooding.

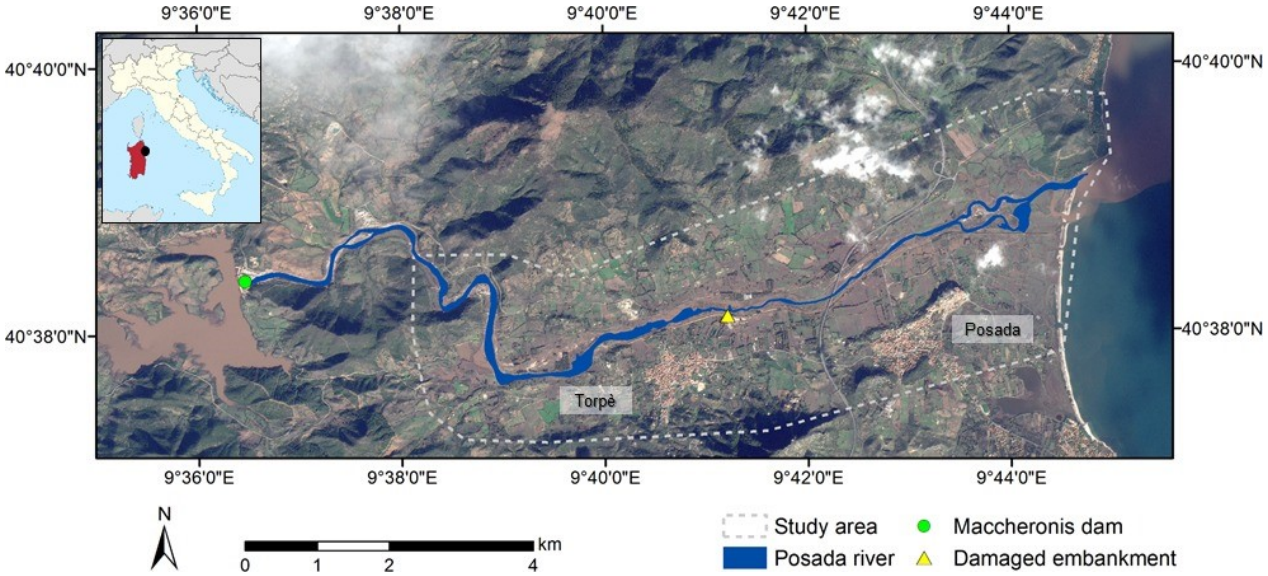

Figure 1 Study area on the SPOT 6 image.

Figure 2 The Maccheronis dam (left) and a portion of the embankment (right) after the flood event.

3. MATERIALS

A four bands post-event SPOT 6 image was provided by ITHACA (Information Technology for Humanitarian Assistance, Cooperation and Action) in the framework of the Copernicus project (Table 1). It was acquired on 21st November 2013, i.e. three days after Cleopatra passing over the Sardinia region.

Table 1 SPOT 6 characteristics.

Acquisition date	21st November 2013
Acquisition time	9:43 A.M
Processing level	Primary
Spectral combination	Pan-sharpened 4 bands (B G R NIR)
Spatial resolution	1.6 m
Product encoding	12 bits
Cloud cover	7%

The 10 m pixel size Digital Terrain Model (DTM) of the Sardinia was used for the SPOT 6 orthorectification along with the Multiprecision DataBase (DBMP) provided by the Sardinia regional authority. Both data were freely collected from the "Sardegna GeoPortale" (http://www.sardegnageoportale.it/).

Damage map, produced by the Copernicus Emergency Management Service (EMS) for the flood event analyzed, was used as independent data to evaluate the results accuracy. In this map, the thematic layers, assessing the delineation of the event, were based on visual interpretation of the SPOT 6 image (Figure 3). The reported thematic accuracy of this map is 60% or better.

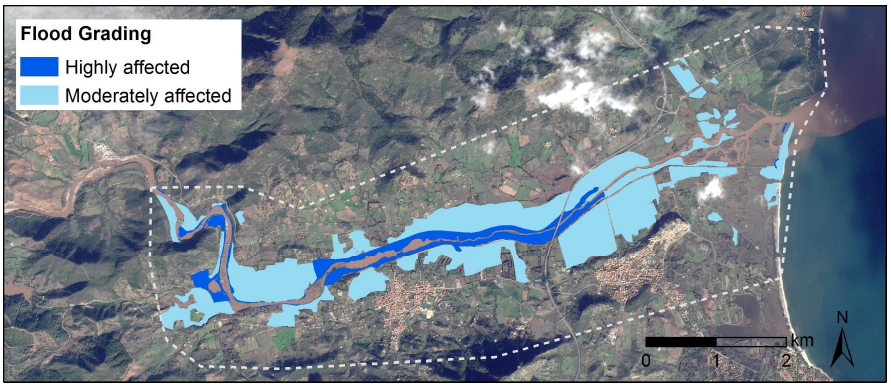

Figure 3 Flood damage grading in the study area.
(source: http://emergency.copernicus.eu/mapping/list-of-components/EMSR061).

4. METHODS

Figure 4 shows the workflow of the study. The post-event image was radiometrically calibrated and orthorectified. Four classification techniques were then applied for mapping the areas covered by water. By means of GIS overlay operation between each "water" class resulting from the four procedures tested and the Posada river vector layer, "flooded areas" vector layer was extracted. The results were compared with flood grading map of Copernicus EMS.

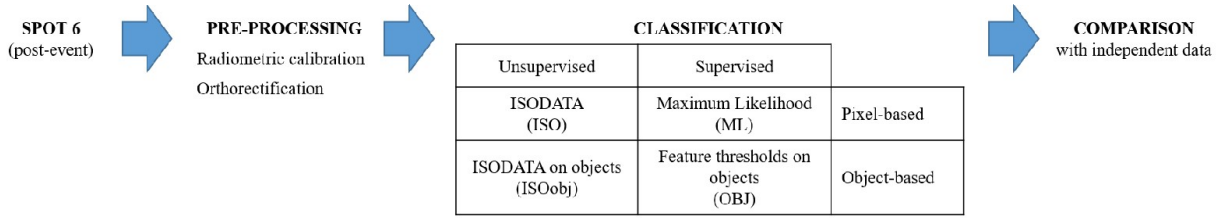

Figure 4 The workflow followed for mapping flooded affected area.

4.1 Image pre-processing

Before performing classification procedures, the SPOT 6 image (60 km x 60 km) was radiometrically calibrated in order to convert the DN values into Top of Atmosphere (TOA) reflectance. The four multispectral bands were orthorectified using the 10 m pixel size DTM before mentioned and selecting six Ground Control Points (GCP) from the DBMP digital cartography. A root mean square error lower than one pixel (0.43) was achieved. The orthorectified image was then resampled to 2 m by a bilinear interpolation. A subset of the image was performed to analyse the downstream of the dam. The software ENVI 5.3 was used for these procedures.

4.2 Image classification

As stated before, a major aim of the work was to evaluate the results of different methods in the image classification, either unsupervised and supervised, using a pixel-based or an object-based approach. A short description of the procedures applied is provided.

4.2.1 ISODATA (ISO)

The unsupervised classification algorithm ISODATA was tested in the perspective of emergency management, when the rapid detection of the flood boundaries is crucial for the response activities such as evacuation, rescue and needs assessment. A maximum of ten classes and five iteration steps were set. The resulting classes were assigned to different land cover categories by photointerpretation. Three classes were interpreted as vegetated areas, two classes were assigned to clouds, one to cultivated lands, one to built-up areas, one class to bare soil and one class appeared to represent salty water. Zones covered by turbid water and wetlands were classified into a single class; however, some urban areas (e.g. streets and zone between buildings) were comprised into this class. To reduce these misclassifications a decision tree approach was performed on the latter class. Thresholds on blue and NDVI bands were applied to remove built-up areas from turbid water and wetland. Finally, the refined class and the salty water class were merged to represent "water" class.

4.2.2 Maximum Likelihood (ML)

Six basic informative classes (Table 2) were identified by photointerpretation and spectral profile analyses, and for each category a number of training sites was selected. Several classes of water were needed to catch the spectral variability and effectively represent the post-event situation. Figure 5 shows some spectral profiles of the water classes. Natural colour, false colour standard and NDVI images were particularly useful for the identification of these classes.

The pixel-based Maximum Likelihood algorithm implemented in ENVI 5.3 was selected for the classification. The four bands of the SPOT 6 and the NDVI were considered, and a probability threshold equal to 0.95 was set. After the classification process, "turbid water", "salt water", "water dam" and "wetland" classes were merged in a single "water" class.

Table 2 ML classification; informative class description.

Informative class	Description
Turbid water	Water with suspended solids and sediment transport (e.g. river, flooded areas)
Salt water	Areas covered by salty water (e.g. sea, lake)
Water dam	Muddy water in correspondence of the Maccheronis dam
Wetland	Areas with high moisture content, potentially flooded
Shadow	Shaded areas, very dark zones
Cloud	Cloud cover

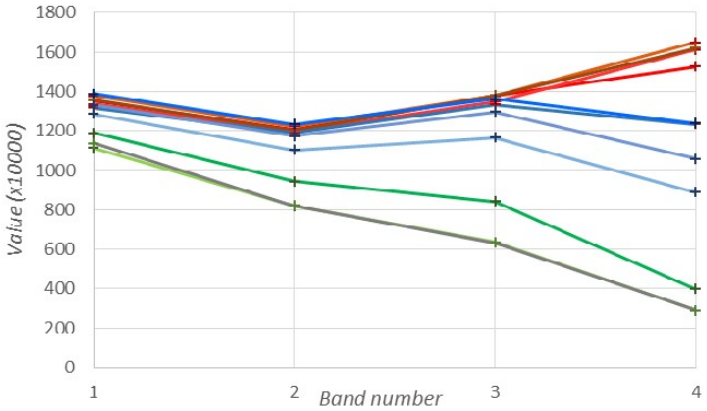

Figure 5 Spectral profiles: green for "salt water", blue for "water dam" and red for "turbid water". (Band number: 1 B, 2 G, 3 R, 4 NIR)

4.2.3 Feature thresholds on objects (OBJ)

The object-based supervised classification was performed on the SPOT 6 with the software eCognition 8.9. This technique consists in two phases; the segmentation, for dividing image into continuous and homogeneous segments, called image objects, and the classification for assigning objects to different categories by using information such as texture, shape, and context[13].

The multiresolution segmentation algorithm, a region growing technique, was used to generate the image objects[14]. Both spectral and shape heterogeneity were taken into account through user-defined colour and shape parameters. A multilevel approach was performed producing each superior objects level by using a higher scale parameter. The aim was the generation of the "optimized" level, i.e. an object level which comprises large segments in homogeneous areas (e.g. flooded areas, outcrops, large vegetated areas, bare soil) and distinctively smaller image objects representing small-scale structures (e.g. buildings, trees, roads etc.) and heterogeneous regions[15]. Classification rules were then applied at the "optimized" level in order to detect areas covered by water. NDVI, Brightness and blue band thresholding were used to classify "water" class objects. A shape rule was applied to refine the results: very small objects belonging to "water" class were assigned to the unclassified.

4.2.4 ISODATA on objects (ISOobj)

The multilevel segmentation approach, followed in the OBJ procedure, was performed to obtain the "optimized" level for each SPOT 6 band. The segmented bands were exported as raster file in order to be processed by means of the ISODATA classification. Therefore, the unsupervised classification was applied on the image objects, characterized by the average reflectance value for each band. A decision tree approach, based on blue and NDVI bands, was performed to

refine turbid water and wetlands image objects (section 4.2.1). ENVI 5.3 software was used for this classification procedure.

4.3 Comparison with independent data

To evaluate the classification methods in term of area and processing time, the flood maps resulting from supervised and unsupervised classification techniques were compared with the grading map produced by the Copernicus EMS (Figure 3).

This comparison was performed in GIS environment. Using an intersection operation between the classification results and the flood damage grading layer, "flooded areas" coherently identified were evaluated in terms of extent. The same procedure was performed to quantify "not flooded areas" correctly recognized, corresponding to no damage. Moreover, commission and omission parameters were computed. By the ratio of the "correctly" classified area, equal to the sum of the flooded and not flooded areas properly identified, and the extent of the study area, the overall accuracy values were calculated for the different classification results; in this case, they must be simply interpreted as a measure of the agreement between the classifications and the independent data source.

The symmetrical difference operation, executed between flooded areas extracted by the classifications and affected areas on the damage grading map, allowed to assess commission error for each classification. In particular, this parameter was computed as the ratio between the results of the symmetrical difference and the "flooded areas" correctly detected. A similar procedure was performed for the omission error; it was calculated by dividing the symmetrical difference between affected areas on the Copernicus EMS map and the "flooded areas" on each classification, with the total affected areas [13].

Table 3 Affected areas in the damage grading map.

affected areas (km^2)	5.773	highly affected	0.996
		moderately affected	4.777
not affected areas (km^2)	22.265		

5. RESULTS AND DISCUSSION

5.1 Image classification: flooded areas

Figure 6 and Figure 7 show the flood maps resulting from each classification technique. Flood affected areas, identified by each classification approach, are listed in Table 4.

In the ML, ISO and ISOobj maps some pixels belonging to streets or building shadows were assigned to floods class. Using geometric information, OBJ classification allowed to avoid some of these misclassification errors. In general, OBJ classification seems to work better than the other techniques in urban areas.

Classification results in correspondence of the damaged embankment prove that both pixel and object-based classification techniques detected well the flooded areas where land is clearly covered by water.

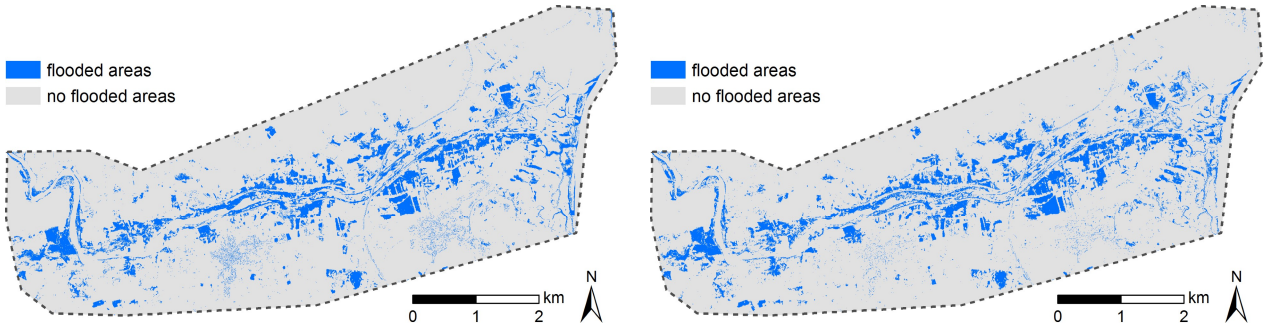

Figure 6 Flooded areas detected by means of ISODATA (left) and Maximum Likelihood (right) classifications.

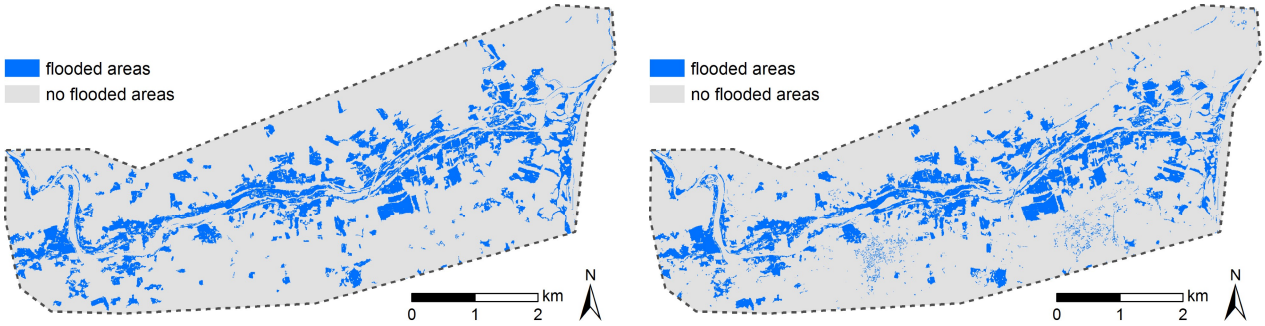

Figure 7 Flooded areas detected by means of object-based classification (left) and the combined object-based and ISODATA approach (right).

Table 4 Flooded areas for each classification approach.

Classification	flooded areas (km^2)	no flooded areas (km^2)
ISO	3.294	24.743
ML	3.252	24.786
OBJ	4.709	23.328
ISOobj	4.468	23.569

5.2 Results of the comparison with independent data

Figure 8 and Figure 9 show the comparison between Copernicus EMS map and ISO and ML classifications and OBJ and ISOobj approaches respectively.

Floods "correctly" detected and commission and omission errors, in terms of area (km^2), are listed in Table 5. OBJ approach achieved the highest values for flooded areas correctly detected followed by the ISOobj approach. These classification techniques resulted in higher commission and lower omission in respect to the pixel based approaches.

Similar accuracy parameters (Figure 10) were obtained for all the results; both pixel and object-based classification techniques can be effectively used to process VHR satellite image for flood mapping purpose.

In a context of rapid mapping, commission errors produce false "alarm" that in post-classification can be reduced by photointerpretation. However, omission errors are more difficult to detect. In order to characterize the omission errors, the flooded areas not detected by each classification were overlaid with the damage grading map. Omission error mainly occurred in correspondence of moderately affected areas (Table 6), confirming that all the classifications detect well the flooded areas where land is completely covered by water, i.e. highly affected areas.

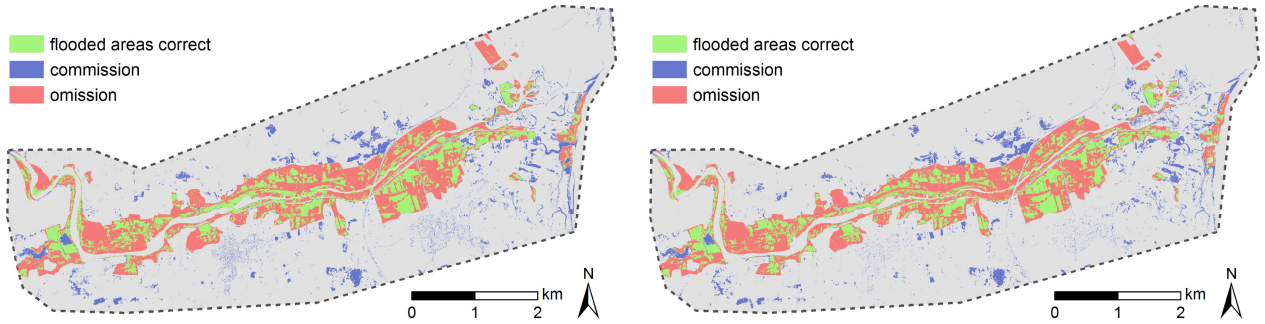

Figure 8 Flooded areas correctly detected and commission and omission resulting from ISODATA (left) and Maximum Likelihood (right) classifications.

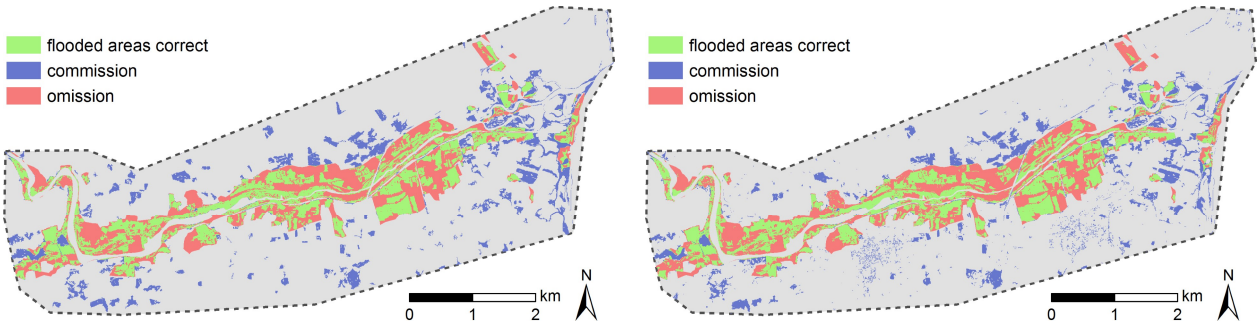

Figure 9 Flooded areas correctly detected and commission and omission resulting from object-oriented classification (left) and the combined object-based and ISODATA approach (right).

Table 5 Results of the comparisons with the grading map.

Classification	**flooded areas correct** (km^2)	**no flooded areas correct** (km^2)	**Commission** (km^2)	**Omission** (km^2)
ISO	2.080	21.047	1.218	3.693
ML	2.088	21.098	1.167	3.685
OBJ	2.845	20.398	1.867	2.927
ISOobj	2.774	20.566	1.698	2.999

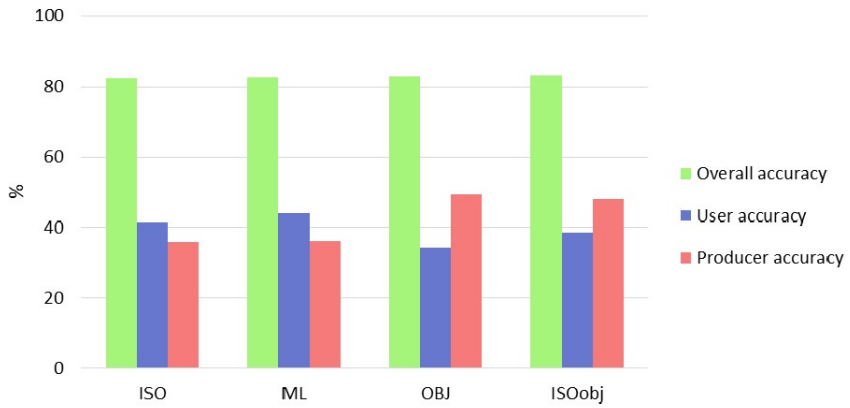

Figure 10 Comparison parameters for each classification approach.

Table 6 Omission statistics.

Classification	highly affected (%)	moderately affected (%)
ISO	13	87
ML	15	85
OBJ	12	88
ISOobj	13	87

6. CONCLUSIONS

VHR satellite images are suitable for pinpointing locations and damages after a flood event. In this work a SPOT6 image was process for flood mapping purpose by using different classification techniques that were compared in terms of results.

In general, supervised classification techniques are considered more accurate than the unsupervised. Results showed, however, that both the approaches can be effectively used to process VHR satellite image for the detection of flooded areas after an extreme event. In fact, when comparing the results with an independent map, similar omission and commission errors were obtained.

Automatic unsupervised procedures required a processing time significantly shorter if compared to the supervised techniques: an important characteristic during the post-event phases when detailed and up-to-date information can support the emergency activities such as evacuation, rescue and needs assessment and damages estimation.

Object-based techniques appeared slightly better than the pixel-based in term of overall agreement with the independent data. It is worth to mention that the process tree developed for the object-oriented approach selecting feature thresholds might be applied on other VHR images. Moreover, the combined object-based and ISODATA approach can be a time reducing alternative with reference to the rules selection and the thresholds definition.

REFERENCES

[1] Münchener Rückversicherungs-Gesellschaft (Munich Re), "NatCatSERVICE Loss events worldwide 2013," München, Germany (2014).

[2] J. Sanyal and X. X. Lu, "Application of Remote Sensing in Flood Management with Special Reference to Monsoon Asia: A Review," Nat. Hazards, 33(2), 283–301 (2004)

[3] Y. Liu, Q. Dai, and J. Liu, "An automatic method for flooded area extraction based on level set method using remote sensing data," IEEE Geoscience and Remote Sensing Symposium, 2142–2145 (2014).

[4] C. Van Westen, "Remote sensing for natural disaster management," Int. Arch. Photogramm. Remote Sens., XXXIII, 1609–1617 (2000).

[5] B. Li and J. Liu, "Application of Remote Sensing Technique for Disaster Management," IEEE International Symposium on Geoscience and Remote Sensing, 283–286 (2006).

[6] F. Franci, E. Mandanici, and G. Bitelli, "Remote sensing analysis for flood risk management in urban sprawl contexts," Geomatics, Nat. Hazards Risk, (6)5–7, 583–599 (2015).

[7] P. Boccardo, "New perspectives in emergency mapping," Eur. J. Remote Sens., 46, 571–582 (2013).

[8] O. M. Bello and Y. A. Aina, "Satellite remote sensing as a tool in disaster management and sustainable development: towards a synergistic approach," Procedia - Soc. Behav. Sci., 120, 365–373 (2014).

[9] M. Haq, M. Akhtar, S. Muhammad, S. Paras, and J. Rahmatullah, "Techniques of Remote Sensing and GIS for flood monitoring and damage assessment: A case study of Sindh province, Pakistan," Egypt. J. Remote Sens. Sp. Sci., 15(2), 135–141 (2012).

[10] F. Franci, G. Bitelli, E. Mandanici, D. Hadjimitsis, and A. Agapiou, "Satellite remote sensing and GIS-based multi-criteria analysis for flood hazard mapping," Nat. Hazards, (2016).

[11] G. Bitelli, F. Franci, and E. Mandanici, "Monitoring the urban growth of Dhaka (Bangladesh) by satellite imagery in flooding risk management perspective," in International Archives of the Photogrammetry, Remote Sensing and Spatial Information Sciences - ISPRS Archives, 40(5W3), 45–50 (2013).

[12] A. Scarsi, W. J. Emery, G. Moser, F. Pacifici, and S. B. Serpico, "An automated flood detection framework for very high spatial resolution imagery," IEEE Geoscience and Remote Sensing Symposium, 4954–4957 (2014).

[13] F. Franci, A. Lambertini, and G. Bitelli, "Integration of different geospatial data in urban areas: a case of study," Proceedings of SPIE, 9229, 92290P1–9 (2014).

[14] M. Baatz and A. Schäpe, "Multiresolution segmentation: an optimization approach for high quality multi-scale image segmentation," in Angewandte Geographische Informationsverarbeitung XII AGIT symposium, 58, 12–23 (2000).

[15] H. Taubenböck, T. Esch, M. Wurm, a. Roth, and S. Dech, "Object-based feature extraction using high spatial resolution satellite data of urban areas," J. Spat. Sci., 55(1), 117–132 (2010).